Alternative lipid synthesis in response to phosphate limitation promotes antibiotic tolerance in Gram-negative ESKAPE pathogens

Roberto Jhonatan Olea-Ozuna[1], Melanie J. Campbell[2], Samantha Y. Quintanilla[1], Sinjini Nandy[1], Jennifer S. Brodbelt[2], and Joseph M. Boll[1, #]

Affiliations:

[1]Department of Biological Sciences, University of Texas at Dallas, Richardson, TX, USA

[2]Department of Chemistry, University of Texas at Austin, Austin, TX, USA

[#]Corresponding Author:

Email: joseph.boll@utdallas.edu

Abstract

The Gram-negative outer membrane protects bacterial cells from environmental toxins such as antibiotics. The outer membrane lipid bilayer is asymmetric; while glycerophospholipids compose the periplasmic facing leaflet, the surface layer is enriched with phosphate-containing lipopolysaccharides. The anionic phosphates that decorate the cell surface promote electrostatic interactions with cationic antimicrobial peptides such as colistin, allowing them to penetrate the bilayer, form pores, and lyse the cell. Colistin is prescribed as a last-line therapy to treat multidrug-resistant Gram-negative infections.

Acinetobacter baumannii is an ESKAPE pathogen that rapidly develops resistance to antibiotics and persists for extended periods in the host or on abiotic surfaces. Survival in environmental stress such as phosphate scarcity, represents a clinically significant challenge for nosocomial pathogens. In the face of phosphate starvation, certain bacteria encode adaptive strategies, including the substitution of glycerophospholipids with phosphorus-free lipids. In bacteria, phosphatidylethanolamine, phosphatidylglycerol, and cardiolipin are conserved glycerophospholipids that form lipid bilayers. Here, we demonstrate that in response to phosphate limitation, conserved regulatory mechanisms induce alternative lipid production in *A. baumannii*. Specifically, phosphate limitation induces formation of three lipids, including amine-containing ornithine and lysine aminolipids. Mutations that inactivate aminolipid biosynthesis exhibit fitness defects relative to wild type in colistin growth and killing assays. Furthermore, we show that other Gram-negative ESKAPE pathogens accumulate aminolipids under phosphate limiting growth conditions, suggesting aminolipid biosynthesis may represent a broad strategy to overcome cationic antimicrobial peptide-mediated killing.

Author Summary

Gram-negative ESKAPE pathogens, including A*cinetobacter baumannii*, are responsible for a dramatic increase in the morbidity and mortality of patients in healthcare settings over the past two decades. Infections are difficult to treat due to antibiotic resistance and tolerance; however, broadly conserved mechanisms that promote antibiotic treatment failure have not been extensively studied. Herein, we identify an alternative lipid biosynthesis pathway that is induced in phosphate starvation that enables Gram-negative ESKAPE pathogens, including *A. baumannii*, *Klebsiella pneumoniae*, and *Enterobacter cloacae* to build lipid bilayers in the absence of glycerophospholipids, which are the canonical bilayers lipid. Replacement of the anionic phosphate in the lipid headgroup with zwitterionic ornithine and lysine promote survival against colistin, a last resort antimicrobial used against Gram-negative infections. These studies suggest that ESKAPE pathogens can remodel their bilayers with phosphate free lipids to overcome colistin treatment and that aminolipid biosynthesis could be targeted to improve antimicrobial treatment.

Introduction

The Gram-negative cell envelope consists of a symmetrical bilayer of glycerophospholipids in the inner membrane, while the outer membrane exhibits an asymmetrical composition, with glycerophospholipids in the periplasmic leaflet and lipopolysaccharide enriched in the outer leaflet (1). The intricate organization underscores the remarkable complexity of bacterial membrane architecture, crucial for microbial survival in various environments. However, under specific stress conditions such as nutrient limitation, temperature fluctuations or exposure to antimicrobial agents, certain bacteria activate alternative lipid biosynthesis pathways or modify existing lipids to adapt and ensure cellular viability (2). One example is aminolipids, which contain amino acid headgroups like lysine, glycine, glutamine, and serine-glycine, with ornithine being the most common (3,4). Ornithine lipids (OLs) are phosphorus-free and found exclusively in bacteria; they are absent in archaea or eukaryotes (5). Their basic structure comprises a 3-hydroxylated fatty acid linked by an amide bond to the α-amino group of ornithine and a second fatty acid attached by an ester bond to the 3-hydroxyl group of the first fatty acid (6). Although OLs are found in both the inner and outer lipid bilayers of Gram-negative bacteria, they are enriched in the outer membrane (7–10). OL biosynthesis is catalyzed by two acyltransferases, OlsB and OlsA, or by the bifunctional acyltransferase OlsF (11–13). In some Gram-negative pathogens such as *Pseudomonas aeruginosa* or *Vibrio cholerae*, OLs are exclusively formed under phosphate limiting conditions (14,15), indicating the presence of a specific regulatory mechanism. The importance of aminolipids transcends basic physiology, especially in the context of antibiotic resistance. ESKAPE pathogens, a group of pathogens that include *Acinetobacter baumannii*, are notorious for their ability to overcome antibiotic treatment and cause hospital-acquired infections (16). Aminolipid synthesis has been implicated in

increased bacterial fitness under antimicrobial stress (9,17,18), potentially contributing to pathogen persistence in clinical settings. Additionally, there is a notable relationship between membrane lipid remodeling and resistance to colistin, a last-resort antibiotic that is used against multi-drug resistant Gram-negative infections (19–22). Chemical modifications to the lipid A domain of lipopolysaccharide or enrichment of amino acid-containing glycerophospholipids have been associated with colistin resistance (23–25), highlighting the importance of understanding lipid metabolism in combating antibiotic resistance.

In this study, we demonstrate that *A. baumannii* produced two aminolipids in limiting phosphate growth conditions, including lysine lipids (LLs) and OLs. OL and LL synthesis is dependent on the *olsB* and *olsA* genes, and *olsB* expression is regulated transcriptionally by the response regulator, PhoR. Additionally, mutants deficient in aminolipid synthesis exhibit increased colistin susceptibility relative to wild type. We also found that other Gram-negative ESKAPE pathogens, including *Klebsiella pneumoniae* and *Enterobacter cloacae*, accumulate aminolipids under phosphate limited growth conditions. These findings suggest a broad survival strategy among ESKAPE pathogens that could promote survival during antibiotic treatment.

Results

Phosphate limitation induces lipid membrane composition modifications in *A. baumannii*

The membrane lipid composition of diverse *A. baumannii* isolates was analyzed, including strains ATCC 17978, ATCC 19606, and AB5075, cultivated in complex lysogeny broth (LB) medium supplemented with ^{32}P-orthophosphoric acid. Labelled cells were collected at mid-logarithmic growth phase, lipids were extracted using the Bligh and Dyer method, and separated by hydrophobicity using two-dimensional thin-layer chromatography (TLC), as previously done (26). We also prepared lipid extracts from well-characterized *Escherichia coli* K-12 strain W3110 for comparison (27). TLC analysis showed conserved glycerophospholipid enrichment corresponding to known structures, including phosphatidylethanolamine (PE), phosphatidylglycerol (PG), and cardiolipin (CL) (**Figure S1A**). Additionally, *A. baumannii* strains also produced two distinct lipid species, including lyso-PE (20) and an unknown phospholipid, denoted as UPL1, that could be a CL derivative, mono-lyso CL (28). The chemical structures of known phospholipids are shown in **Figure S1B**.

A. baumannii strain ATCC 17978 cultured in minimal medium with 1 mM (excess) phosphate displayed a lipid composition almost equivalent to growth in complex LB medium (**Figure 1 and Figure S1A**). One notable change was that UPL1 was absent, and another unidentified lipid, denoted as UPL2, was formed, likely representing another CL derivative. To explore lipid biosynthesis under phosphate-limiting condition, membrane lipid profiles were analyzed after growth in minimal media supplemented with 50 μM (limiting) phosphate concentrations (**Figure 1**). Limited phosphate availability impacted relative lipid levels, suggesting decreased phosphate-containing lipid synthesis. Concomitant production of three

145 unknown lipids, referred to as unknown lipids 1 (U1), 2 (U2), and 3 (U3), were produced in
146 phosphate limiting growth. Ninhydrin staining revealed that U1 and U2 contained free
147 amines, like PE. Increased ratios of ninhydrin-stained unknown aminolipids relative to PE
148 showed that under phosphate-limiting conditions, potential phosphate-free aminolipids were
149 produced.

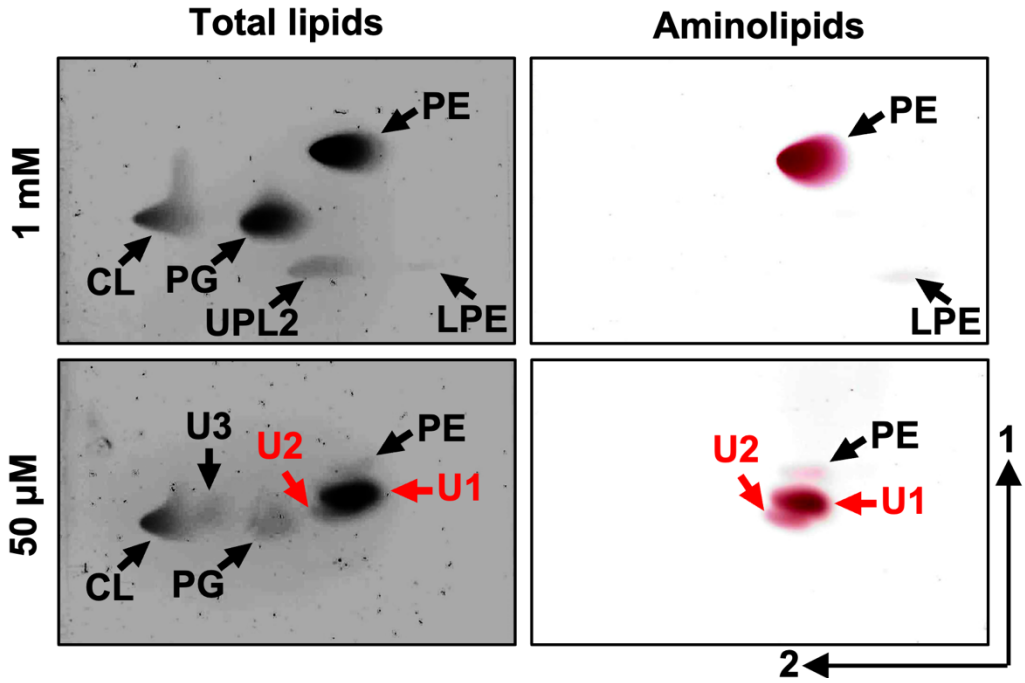

Figure 1: Lipid composition of *A. baumannii* strain ATCC 17978 in excess and limiting phosphate concentrations. Strains were grown in minimal with excess (1 mM) or limiting (50 µM) phosphate. Cells were collected, lipids were extracted using the Bligh and Dyer method and separated using 2-dimensional thin-layer chromatography. Total lipids were stained with sulfuric acid (left). Aminolipids were stained using ninhydrin (right). Specific lipids are labelled: PE, phosphatidylethanolamine; PG, phosphatidylglycerol; CL, cardiolipin; LPE, lyso-PE; U1, unknown lipid 1; U2, unknown lipid 2; U3, unknown lipid 3; UPL2, unknown phospholipid 2. Red letters denote aminolipids that provide the focus of the study.

158 Growth in limiting phosphate concentrations slowed growth in ATCC 17978 relative
159 to excess phosphate (**Figure S2A**), and microscopic analysis revealed that cells elongated
160 and increased their surface area when phosphate is limiting (**Figure S2B and S2C**), a
161 response previously reported in other Gram-negative bacteria (29). Additionally, while the
162 composition of lipooligosaccharide (LOS) fractions remained consistent across limiting

phosphate conditions, the relative level of LOS was decreased under phosphate limitation (**Figure S2D**).

Aminolipids synthesized during phosphate limitation are OLs and LLs

One dimensional TLC showed three lipids (PE, U1, and U2) stained with ninhydrin (**Figure S3A**). After separation of lipids based on hydrophobicity, individual bands corresponding with U1 and U2 were scraped from the TLC plates and extracted using the Bligh and Dyer method. U1 and U2 bands were analyzed by liquid-chromatography mass spectrometry (LC-MS) and structurally characterized using tandem mass spectrometry (MS/MS) (**Figure 2**). The elution profiles obtained for the U1 and U2 bands are displayed in **Figures 2A** and **2D,** respectively. To determine the composition of aminolipids, a data-dependent acquisition method was used to isolate and activate the most abundant ions detected in each chromatographic peak with higher energy collisional dissociation (HCD) in negative-ionization mode. HCD of precursor *m/z* 621.52 found in the U1 extract resulted in the loss of the headgroup, which was observed at *m/z* 131.08, and corresponded to deprotonated ornithine (**Figure 2B**). The most abundant fragment ion (*m/z* 367.30) was used to identify the acyl chain connected to the headgroup as 16:0 (number of carbon atoms: double bonds). Further, the complementary ion of *m/z* 253.22 confirmed the identity of the fatty acid connected at the 3-hydroxyl position of the first fatty acid as 16:1. Following this analysis, lipids containing a double bond were subsequently targeted in second LC run in the positive-ionization mode using 193 nm ultraviolet photodissociation (UVPD) for MS/MS. UVPD is an alternative fragmentation method that utilizes high-energy photons to activate and dissociate the selected lipid precursor ions, allowing localization of the double bonds within the fatty acyl chains. UVPD of precursor *m/z* 623.53 produced two fragment ions

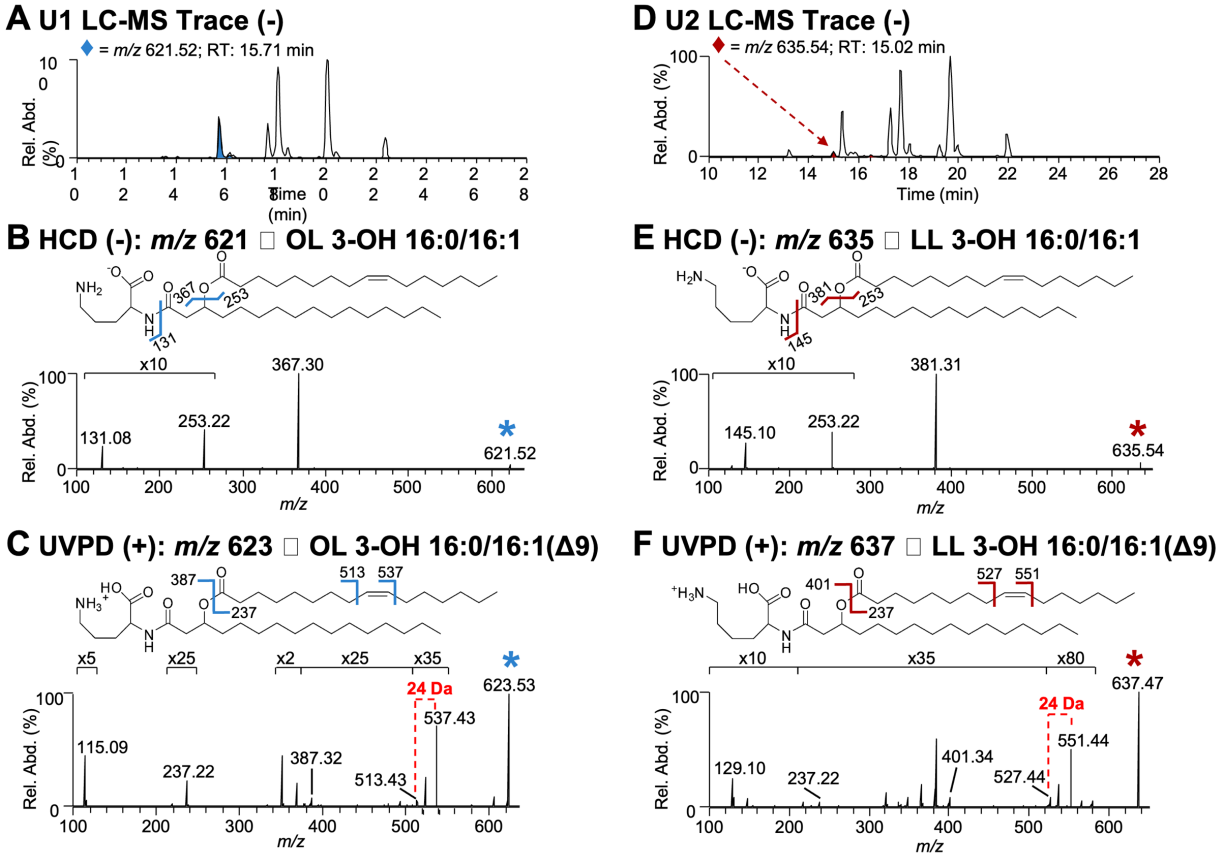

Figure 2: Structural analysis of the lipids produced during phosphate limitation. A. LC-MS trace of U1 lipid extract in negative ionization mode. **B.** HCD (NCE 22) mass spectrum of *m/z* 621.52 ($[M-H]^-$), an ornithine lipid found in U1 extract**. C.** UVPD (4 pulses at 2 mJ/pulse) mass spectrum of *m/z* 623.53 ($[M+H]^+$). **D.** LC-MS trace of U2 lipid extract in negative ionization mode. **E.** HCD (NCE 22) mass spectrum of *m/z* 635.54 ($[M-H]^-$), a lysine lipid found in U2 extract. **F.** UVPD (4 pulses at 2 mJ/pulse) mass spectrum of *m/z* 637.47 ($[M+H]^+$). The selected precursor ions are labeled with asterisks in B,C,E,

separated by 24 Da that originate from cleavages adjacent to the double bond. This pair of diagnostic ions localizes the double bond to the 9th position (**Figure 2C**). This LC-MS/MS strategy identified 49 OLs, including double bond isomers, and 10 unknown lipids in the U1 extract (**Table S1**) and a total of 24 OLs and 16 unknown lipids in the U2 extract (**Table S2**). HCD of the unknown lipids yielded similar fragmentation to that observed for OLs, but the fragmentation patterns were distinguished by the release of a deprotonated headgroup that corresponded to either a lysine or monomethylated ornithine headgroup (*m/z* 145.10) (**Figure 2E**). While the aminolipid head group could be either lysine or monomethylated ornithine, the absence of an ortholog for OlsG, the enzyme responsible for OL methylation (30), and

196 the presence of *olsG* only in certain planctomycete genomes, strongly suggests that OL
197 methylation is unlikely to occur in *A. baumannii*. Therefore, the identified lipid is denoted
198 herein as a LL.

199 After confirming that *A. baumannii* strain ATCC 17978 produces OLs and LLs, we
200 explored if other *A. baumannii* isolates form these aminolipids during phosphate limitation.
201 One-dimensional TLC stained with ninhydrin revealed that diverse *A. baumannii* strains,
202 including ATCC 17978, ATCC 19606, AB5075, AYE, and the environmental isolate, *A.*
203 *baylyi*, were also capable of aminolipid biosynthesis in response to phosphate limitation
204 (**Figure S3B**). Together, these studies suggest that *Acinetobacter* can form lipid bilayers with
205 not only glycerophospholipids, but also membranes enriched with OLs and LLs when
206 phosphate availability is limited.

207

208 **Differentially regulated genes during phosphate starvation**

209 To determine genes that regulate aminolipid biosynthesis, total RNA was isolated,
210 rRNA was depleted, and transcripts were sequenced from *A. baumannii* strain ATCC 17978
211 after growth in minimal media supplemented with 1 mM (excess) and 50 μM (limiting)
212 phosphate. Using a cutoff of 3-fold weighted proportions fold change with an FDR p-
213 value correction < 0.05, 67 upregulated genes and 109 downregulated genes were found
214 (**Figure 3A**). Many down-regulated genes were involved in iron uptake and lysine
215 degradation. Upregulated genes included pathways involved in TAT-dependent proteins
216 export, phospholipases, lipid metabolism, regulation and phosphate transporters. A complete
217 list of significant ($P < 0.05$) up- and down-regulated genes is included in **Table S3**.

One notable up-regulated gene (*A1S_0889*) showed 31% identity and 51% similarity (91% coverage) to *P. aeruginosa olsB*. While not induced in phosphate starvation, *A. baumannii* also encodes a putative *olsA* orthologue (*A1S_2990*) with 43% identity and 61% similarity (78% coverage) to *P. aeruginosa olsA*. OlsBA has been characterized in several bacteria and is involved in OLs biosynthesis (8,11,12,14,31). Notably, *A. baumannii olsA* is

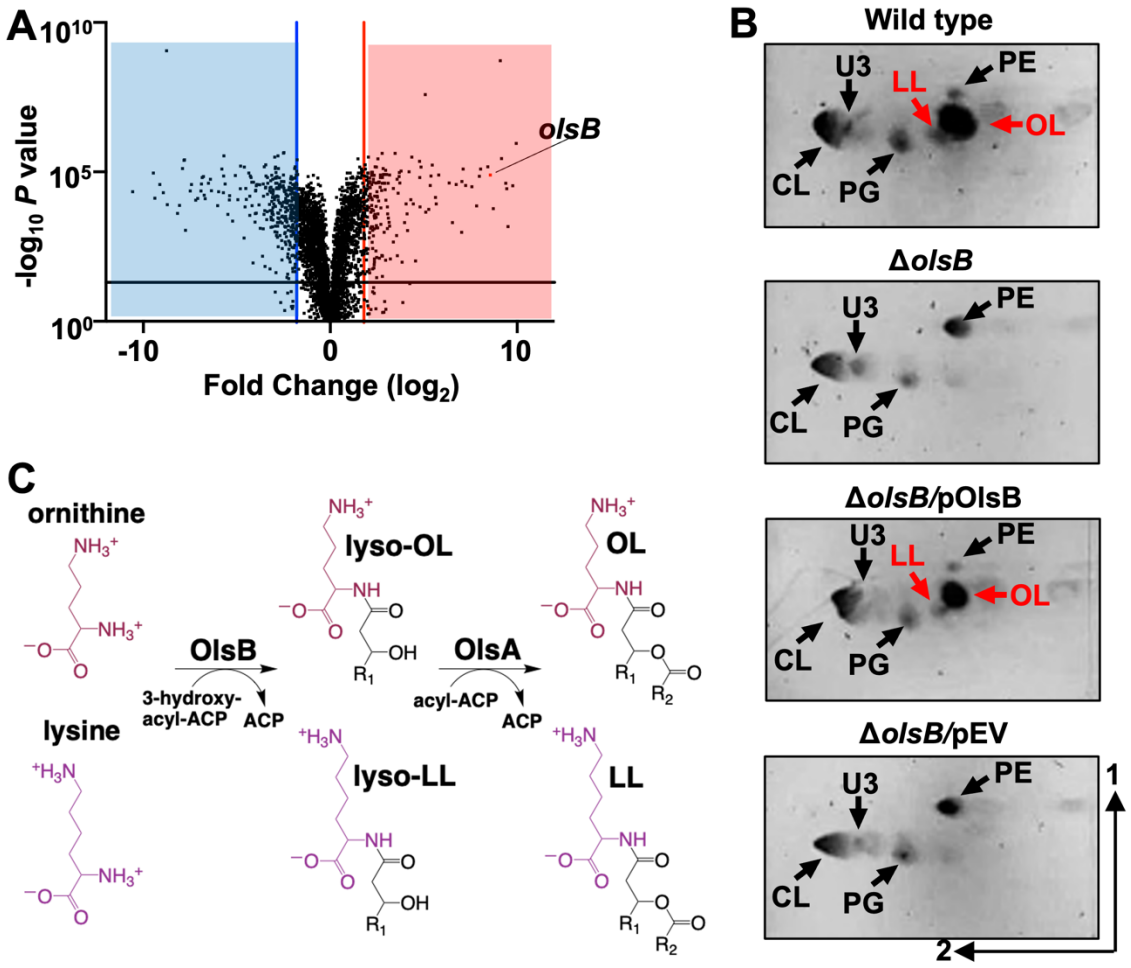

Figure 3: The *olsB* gene is required for ornithine and lysine lipid formation in phosphate limited growth conditions. A. Volcano plot of differentially regulated genes in excess and limiting phosphate. Red/blue lines indicate 3-fold cutoffs. The Black line on the *x*-axis indicates $P < 0.05$. A red dot representing the *olsB* expression profile is shown. **B.** 2D thin-layer chromatography stained with sulfuric acid showing wild type and Δ*olsB* strains grown in phosphate limiting (50 μM) conditions. Specific lipids are labelled: PE, phosphatidylethanolamine; PG, phosphatidylglycerol; CL, cardiolipin; OL, ornithine lipid; LL, lysine lipid; U3, unknown lipid 3. OL and LL aminolipids are labelled in red. **C.** Proposed ornithine lipid (OL) and lysine lipid (LL) biosynthesis pathways in *A. baumannii*.

223 located at a distinct site on the chromosome relative to *olsB* and is not transcriptionally
224 regulated by phosphate concentrations.
225
226 **_olsB_ and _olsA_ genes are required for aminolipids synthesis in _A. baumannii_**
227 Differential gene expression analysis indicated changes in gene dosage in response to
228 excess/limiting phosphate concentration. Specifically, *A1S_0889* expression increased in
229 response to phosphate limitation, whereas *A1S_2990* expression did not change. To confirm
230 that *A1S_0889* was an *olsB* orthologue, we generated Δ*olsB* in *A. baumannii* strain ATCC
231 17978, by fusing codon 33 and 215. TLC analysis revealed that under phosphate limitation,
232 aminolipids were absent in the *olsB*-deficient mutant and a mutant carrying only the empty
233 vector but wild-type accumulated OLs and LLs (**Figure 3B**). Furthermore, *olsB*
234 complementation from a non-native promoter restored OL and LL formation. Based on the
235 lipid migration patterns in wild type, the lipids are OLs and LLs.
236 Additionally, we generated Δ*olsB* (HMPREF0010_01383) in strain ATCC 19606 and
237 analyzed the *olsB::tn* and *olsA::tn* mutants for the AB5075 transposon mutant library (32) in
238 the respective genes, ABUW_3039 and ABUW_0502. Lipid analysis when the mutants were
239 cultivated under phosphate limitation showed that the wild-type strains ATCC 19606 and
240 AB5075 produced OLs and LLs, while the *olsB* and *olsA* mutants did not (**Figure S4A and**
241 **S4B**). The *olsA*::*tn* mutant lipid profile did not show the expected accumulation of lyso-
242 aminolipids, consistent with findings in other Gram-negative Δ*olsA* mutants (33). This
243 suggests that lyso-aminolipids are tightly regulated and rapidly degraded within the cell.
244 These data suggested that ornithine and lysine lipid biosynthesis in *A. baumannii* is
245 dependent on OlsB and OlsA.

Together, this data supports a model suggesting that aminolipid synthesis occurs in at least two distinct steps within *A. baumannii* (**Figure 3C**). Initially, ornithine and lysine undergo acylation in an OlsB-dependent reaction, leading to the formation of lyso-OL and lyso-LL. Subsequently, in a second step facilitated by OlsA, lyso-OL and lyso-LL are further acylated at the hydroxy position, yielding OL and LL, respectively.

Microscopic analysis and comparison of LOS fractions and levels between aminolipid-producing and aminolipid-deficient *A. baumannii* strains revealed no significant morphological differences (**Figure S4C and S4D**) or changes in LOS fractions and relative levels (**Figure S2D)**. However, it is noteworthy that the core fraction of LOS from *A. baumannii* strains ATCC 19606 differs from of the ATCC 17978 or AB5075 strains. Additionally, a faint band in the core fraction was observed in the *olsA*::*tn* transposon mutant of AB5075, which was not present in the wild type strain.

Mutants deficient in aminolipids synthesis show differential growth rate under phosphate limitation

To assess growth rates under phosphate limitation, wild-type and *olsB* mutant strains were grown in minimal medium with limiting phosphate concentrations (**Figure S4E**). The optical density at 600 nm (OD_{600}) was monitored over time. While growth of strain ATCC 17978 Δ*olsB* was not impacted, the growth rate in strains ATCC 19606 and AB5075 was reduced in the *olsB* or *olsA* Tn*101*mutants, suggesting there are strain-dependent effects on aminolipid biosynthesis that impact fitness.

Aminolipid biosynthesis mutants are defective in colistin tolerance

Changes in lipid composition could alter the physicochemical properties of the bilayers, particularly the charge. To explore this concept, the impact of aminolipids biosynthesis on colistin tolerance was measured in *A. baumannii* strain ATCC 17978, where growth rate was not impacted in the *olsB* mutant (**Figure S4E**). Colistin is a cyclic peptide that directly engages with the negative membrane charge, while the hydrophobic tail forms pores, leading to bactericidal activity. Colistin is a last resort antibiotic used against multidrug resistant Gram-negative bacterial infections. Our studies indicate increased colistin susceptibility in the *olsB*-deficient mutant relative to the wild-type strain (**Figure 4A and**

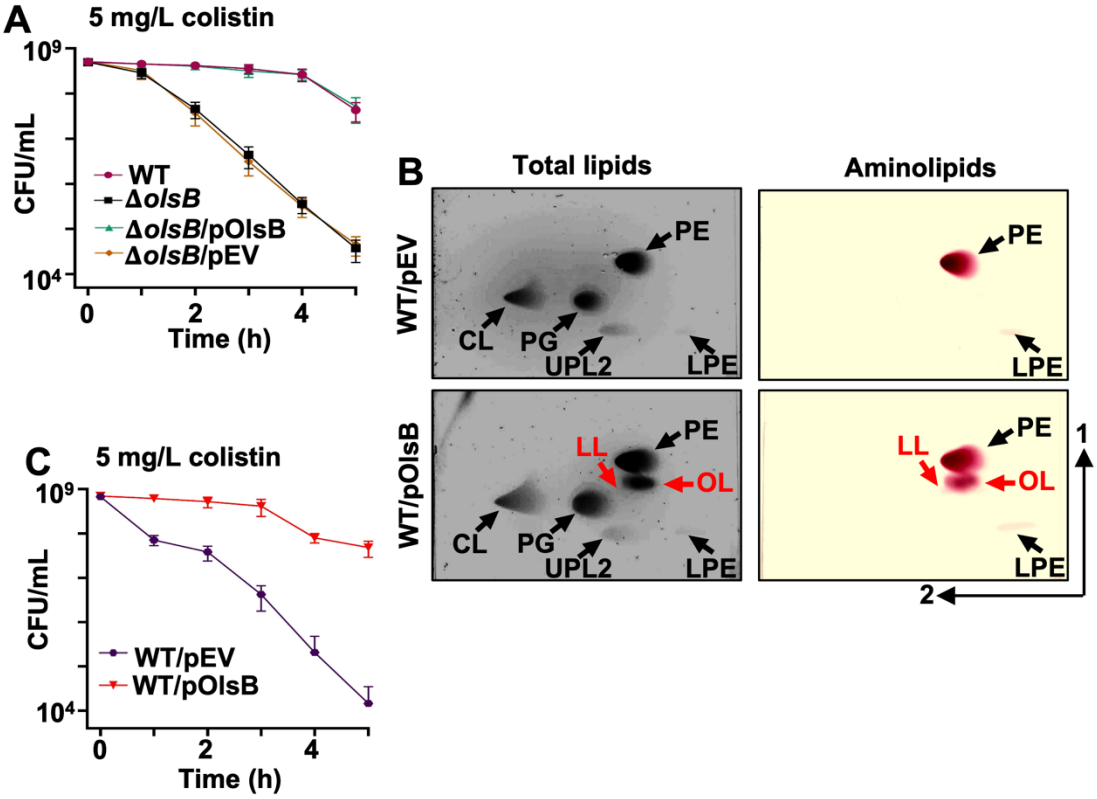

Figure 4: Aminolipids promote colistin tolerance in *A. baumannii*. **A.** Colistin-dependent killing in wild type and Δ*olsB* mutant strains. $n = 3$. Error bars indicate standard deviation. Wild type (WT) strains carrying pOlsB or empty vector were subjected to 5 mg/L colistin exposure over time. CFU/mL were calculated every 0.5 h. **B.** Total lipids were extracted using the Bligh and Dyer method and separated using 2D thin-layer chromatography. Lipids were stained with sulfuric acid (left). Aminolipids were stained using ninhydrin (right). Specific lipids are labelled: PE, phosphatidylethanolamine; PG, phosphatidylglycerol; CL, cardiolipin; LPE, lyso-phosphatidylethanolamine; LL, lysine lipid; OL, ornithine lipid; U3, unknown lipid 3. OL and LL are labelled in red. **C.** Colistin-dependent kill curves (left) and growth rate analysis (right) in wild type expressing empty vector (pEV) or pOlsB ($n = 3$). Error bars indicate standard deviation.

277 **Figure S5A**), suggesting the antibiotic could be more effective against *A. baumannii* when
278 aminolipid biosynthesis is inhibited. Overexpression of *olsB* in wild-type *A. baumannii* was
279 sufficient to produce aminolipids during cultivation in excess phosphate (**Figure 4B**).
280 Analysis demonstrated that *olsB* induction led to increased colistin tolerance (**Figure 4C and**
281 **Figure S5B**). Therefore, OlsB-dependent aminolipid biosynthesis in *A. baumannii* promotes
282 colistin tolerance, a last-line antibiotic for combating multidrug-resistant Gram-negative
283 bacteria.
284
285 **PhoR regulates aminolipid biosynthesis in *A. baumannii***
286 Previous work established that aminolipid production generally occurs in response to
287 phosphate limitation (6,14,15,34,35). Consequently, we expected to find a Pho box upstream
288 of the putative *olsB* gene. Using the *E. coli* pho box consensus sequence (36), a putative Pho
289 box was identified that precedes the *olsB* gene in diverse *Acinetobacter* isolates, including

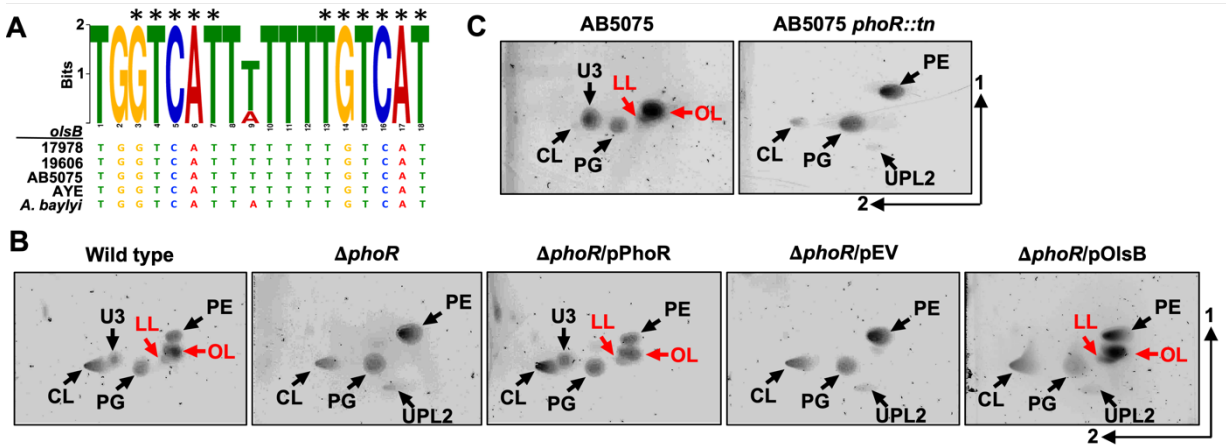

Figure 5: PhoR regulates *olsB* gene expression and aminolipid formation in *A. baumannii* strains. **A.** Predicted Pho box sequence alignments from *A. baumannii* strain 17978, 19606, AB5075, AYE, and *A. baylyi olsB* promoters. Black asterisks represent conserved nucleotides in the *E. coli* Pho box consensus (CT*GTCAT*NNNNC*TGTCAT*). **B.** 2D thin-layer chromatography lipid analysis from *A. baumannii* strain ATCC 17978 wild type and mutants grown in minimal media supplemented with 50 µM (limiting) phosphate. **C.** 2D thin-layer chromatography lipid analysis from *A. baumannii* strain AB5075 wild type and the *phoR* Tn*26* mutant in minimal media supplemented with 50 µM (limiting) phosphate. Lipids were stained with sulfuric acid. OL and LL aminolipids are labelled in red.

290 ATCC 17978 (**Figure 5A**), but not preceding the *olsA* gene. These results are consistent with
291 our transcriptomics analysis, which also suggested *olsA* gene expression is not responsive to
292 phosphate concentrations.

293 Phosphate sensing and diverse responses are regulated by the two-component system,
294 PhoB/PhoR, in many bacteria (37). When phosphate levels decrease, the sensor kinase, PhoR,
295 becomes activated, leading to autophosphorylation. Subsequent phosphotransfer to the
296 cognate response regulator, PhoB results in a conformational change and DNA binding (38)
297 at target promoters to induce gene expression.

298 These findings imply that the PhoB/PhoR two-component system regulates OL and
299 LL biosynthesis in *A. baumannii* through *olsB* expression. To validate this hypothesis, we
300 generated Δ*phoR* (*A1S_3376*) in *A. baumannii* ATCC 17978 by fusing codon 65 to 410. Lipid
301 analysis after growth limiting phosphate, showed that the Δ*phoR* mutant accumulates
302 glycerophospholipids PE, PG, CL, and UPL2, while failing to synthesize OL, LL, and U3,
303 unlike the wild-type strain (**Figure 5B**). Complementation of the *phoR*-deficient mutant with
304 the PhoR allele restored OL and LL formation, while aminolipids were absent in the mutant
305 carrying the empty vector. Expression of *olsB* from a non-native locus in the Δ*phoR* mutant
306 restored OL and LL biosynthesis. Additionally, we examined the lipid patterns of the *phoR*
307 (ABUW_0105)-transposon mutant of *A. baumannii* AB5075 grown under phosphate
308 limitation (**Figure 5C**). Lipidomic analysis revealed that, unlike the wild-type strain, the
309 *phoR::tn* mutant predominantly accumulated phospholipids and was unable to produce OL
310 or LLs. Together, these findings suggest that *olsB* expression in *A. baumannii* is mediated by
311 the *phoR* regulatory gene.
312

Other Gram-negative ESKAPE pathogens form aminolipids under conditions of phosphate depletion

In addition to *P. aeruginosa* (14), *A. baumannii* is the second Gram-negative ESKAPE bacterium where the OL biosynthesis has been described using a OlsBA-dependent mechanisms. Uniquely, *A. baumannii* also produces LL via the same pathway. These findings prompted us to investigate if other Gram-negative ESKAPE pathogens, such as *Klebsiella* or *Enterobacter*, are also capable of aminolipid biosynthesis under phosphate limitation. TLC analysis of total lipids from *K. pneumoniae*, *E. cloacae* or *P. aeruginosa* after growth in minimal medium supplemented with excess phosphates showed production of the canonical

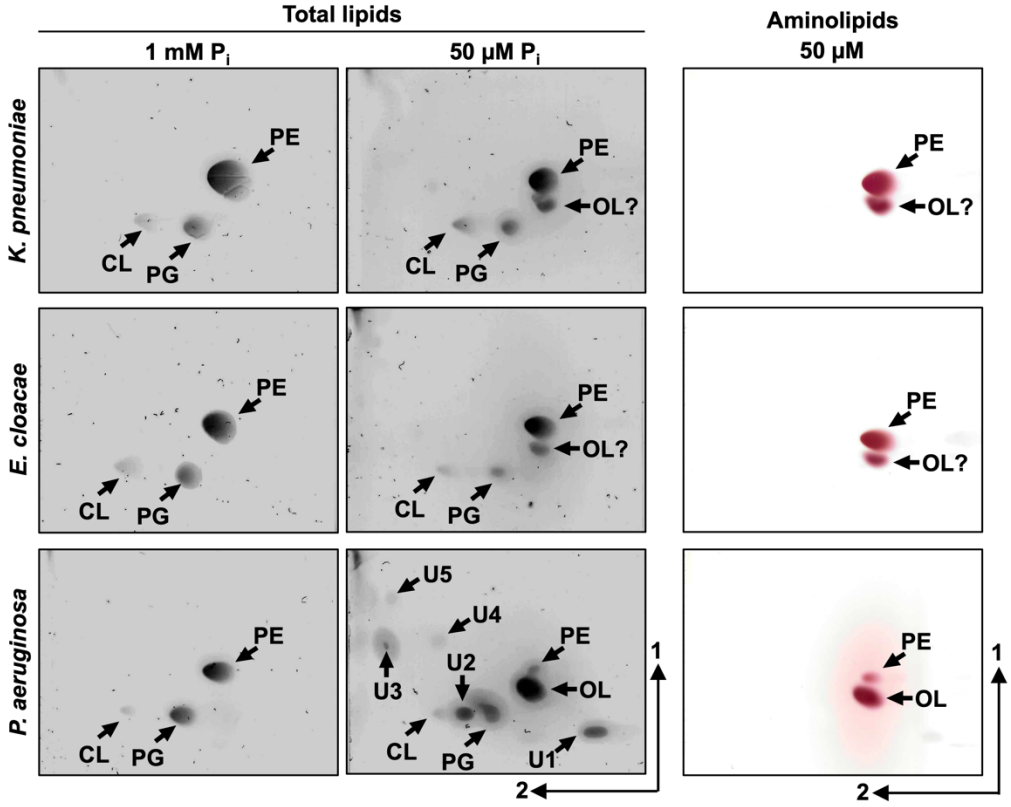

Figure 6: Aminolipid biosynthesis is conserved in Gram-negative ESKAPE pathogens. 2D thin-layer chromatography of lipids extracted from wild type *K. pneumoniae* strain KPNIH1, *E. cloacae* strain ATCC 13047, and *P. aeruginosa* strain PAO1 grown in excess (1 mM) or limiting (50 µM) phosphate conditions. Totals lipids were stained with sulfuric acid (left). Aminolipids were stained using ninhydrin (right). Specific lipids are labelled: PE, phosphatidylethanolamine; PG, phosphatidylglycerol; CL, cardiolipin; OL, ornithine lipid; U1, U2, U3, U4, and U5; unknown compounds 1, 2, 3, 4, and 5.

membrane phospholipids PE, PG, and CL (**Figure 6**). However, when cultivating *P. aeruginosa* in phosphate limitation (50 μM), a significant decrease in relative phospholipid levels was observed, and the synthesis of five unknown compounds and OL was induced. *K. pneumoniae* and *E. cloacae* cultivated in low phosphate concentrations (50 μM), also showed decreased levels of phospholipid production and accumulation of an unknown lipid. The unknown lipid exhibited a migration pattern and ninhydrin staining on TLC like OL, suggesting that aminolipid biosynthesis may be a conserved response to phosphate limiting growth conditions that could promote tolerance to antibiotics in Gram-negative ESKAPE pathogens.

Discussion

Bacteria have evolved various regulatory mechanisms to sense and adapt to environmental stress. Here, we show that under phosphate-limiting conditions, *A. baumannii* produces ornithine and lysine lipids through regulated expression of *olsB*. The aminolipids alter the lipid bilayer composition to promote tolerance to colistin, an antimicrobial peptide used to treat Gram-negative bacterial infections. Specifically, aminolipids could reduce the electrostatic potential for cationic antimicrobial peptides such as colistin to target the cell, emphasizing changes in bilayer charge as an adaptive mechanism for *A. baumannii* in challenging environments. Broadly, cell membrane lipid modifications are vital for bacterial survival upon exposure to antimicrobial cationic peptides. For example, *V. cholerae* modifies lipid A with glycine or diglycine residues to resist cationic antimicrobial peptides (39). Similar strategies are employed by various bacterial species, such as *P. aeruginosa*, *Rhizobium tropici*, *Staphylococcus aureus*, *Mycobacterium tuberculosis*, and *Bacillus*

345 *subtilis*, which modify phospholipids like PG by adding amino acids like lysine or alanine,
346 thereby conferring polymyxins resistance (34,35,40–42).

347 Membrane lipid remodeling during growth under phosphate limitation is a conserved
348 strategy across bacteria, involving the substitution of phospholipids with phosphorus-free
349 lipids alternatives like aminolipids (43). While the synthesis of these lipids is not directly
350 induced by the presence of polymyxins, tolerance to polymyxins is an indirect consequence
351 of lipid membrane remodeling, leading to significant changes in membrane chemical
352 properties. The alteration could reduce the net negative charge of the membrane, thereby
353 decreasing CAMP susceptibility.

354 The *olsB* gene is required for OL biosynthesis, but unlike other OlsB-dependent
355 pathways, it also induces LL formation in *A. baumannii*, suggesting metabolic plasticity
356 within the species. Comparing our findings with observations in other bacteria, such as the
357 soil bacterium *Rhodobacter sphaeroides*, which not only produces OLs but also synthesizes
358 glutamine lipids (GLs) (44), further highlights the metabolic diversity in aminolipid
359 biosynthesis. Additionally, recent research has shown that marine bacteria *Ruegeria*
360 *pomeroyi* encode two *olsB* paralogs, one responsible for forming OLs and the other for GLs
361 (33). Although these bacteria inhabit vastly different environments, the similarities suggest
362 that the ability to use multiple substrates for aminolipid synthesis may be a common survival
363 strategy in variable environmental conditions.

364 The transcriptomic analysis uncovered insights into different expression patterns of
365 the *olsB* and *olsA* genes in response to phosphate limitation. Specifically, overexpression of
366 the *olsB* gene was observed during phosphate limited growth, indicating a regulatory
367 mechanism. However, *olsA* expression remained unchanged. The predicted Pho box in the
368 promoter region of *olsB* suggested that the PhoB/PhoR two-component system regulates *olsB*

under phosphate limitation conditions. Conversely, the absence of a similar motif in the promoter region of *olsA* implies the influence of other regulatory factors on its expression, independent of phosphate availability. Furthermore, *olsB* overexpression with non-native promoter in *A. baumannii* during cultivation in excess phosphate resulted in aminolipid formation, suggesting OlsA-dependent activity occurs after OlsB has formed a lyso-aminolipid. The differential regulatory events may also suggest that OlsA utilizes other substrates. For instance, in *Rhodobacter capsulatus*, OlsA functions as a bifunctional enzyme, active in both OL and phosphatidic acid biosynthesis (45). Additionally, we confirmed the role of the *phoR* gene as a key regulator in aminolipid biosynthesis in *A. baumannii*, highlighting its fine-tuned regulation in response to environmental stressors such as phosphate limitation. Interestingly, this regulatory mechanism shares similarities with species like *Sinorhizobium meliloti* or *V. cholerae*, where PhoB/PhoR also regulates OLs synthesis under phosphate limitation conditions (6,15), underscoring the evolutionary conservation of these adaptive mechanisms across different bacterial taxa.

Finally, the presence of *olsB* and *olsA* orthologues in *A. baumannii* raises questions about the diversity of aminolipid biosynthesis pathways among pathogens. Interestingly, bacteria such as *Klebsiella* and *Enterobacter* lack these orthologs, suggesting distinct biosynthesis pathways compared to *A. baumannii*. This absence prompts further investigation into alternative pathways or genes involved in aminolipid synthesis and their implications for antibiotics resistance and environmental adaptation.

Conclusion

The study highlights the impact of phosphate limitation on lipid membrane composition in *A. baumannii*, resulting in the synthesis of OLs and LLs through regulated

393 *olsB* gene expression. Aminolipids can promote tolerance to colistin, an important last-line
394 antimicrobial. These results also underscore the role for *phoR* gene in regulating aminolipid
395 synthesis in *A. baumannii* and show that other Gram-negative ESKAPE pathogens produce
396 aminolipids under phosphate-depleted conditions. Aminolipid biosynthesis is a common
397 adaptive response to phosphate limitation, which could promote pathogen survival both in
398 hospital environment and within the host.
399
400 **Materials and methods**
401 **Bacterial strains and growth.** All strains and plasmids used in this study are listed in Table
402 S4 in the supplemental material. *E. coli*, *Acinetobacter* strains, *K. pneumoniae*, *E. cloacae* or
403 *P. aeruginosa* were initially cultured from frozen stocks on Luria-Bertani (LB Miller) agar at
404 37ºC. Isolated colonies were used to inoculate LB Miller broth or minimal medium (Tris
405 minimal succinate [TMS]) (46); supplemented with different phosphate concentrations at
406 37ºC. The minimal medium included: Na-succinate 20 mM, NaCl 200 mg/mL, NH_4Cl 450
407 mg/mL, $CaCl_2$ 200 mg/mL, KCl 200 mg/mL, $MgCl_2$ 450 mg/mL, $FeCl_2$ 10 mg/L, and $MnCl_2$
408 10 mg/L, with 10 mM 4-(2-hydroxyethyl)-1-piperazineethanesulfonic acid (HEPES) buffer
409 used at pH 7.2. Na_2HPO_4 was then added to achieve a final concentration of 1 mM (excess)
410 or 50 µM (limiting). All components were dissolved in deionized water and sterilized by
411 filtration trough 0.22 µm pore-size filters and dissolved deionized H_2O. To generate growth
412 curves, overnight cultures of *A. baumannii* strains were diluted to an OD_{600} of ~0.05 in 5 mL
413 of medium, then incubated in glass test tubes at 37ºC for 24 hours. Growth curve data were
414 analyzed and plotted using GraphPad Prism software.
415

Construction of mutant and complementation *A. baumannii* strains. The primers utilized in this study are listed in Table S5 in the supplementary material. Genetic mutants of *A. baumannii* were generated following established protocols (47–50). Briefly, *A. baumannii* carrying the pMMB67EH^{TetR} plasmid containing the REC$_{Ab}$ coding sequences was diluted from an overnight culture into LB Miller broth containing 10µg/mL of tetracycline at an OD_{600} of ~0.05 and incubated for 45 minutes. REC$_{Ab}$ expression was induced by adding 2 mM IPTG, and cells were cultured at 37ºC until they reached mid-log growth phase (OD_{600} of ~0.4). After washing the cells three times in ice-cold 10% glycerol, 10^{10} cells were electroporated in a 2-mm cuvette at 1.8 mV with 5 µg of a recombineering linear PCR product. Subsequently, the cells were cultured for 4 hours in 4 mL of LB Miller broth with 2 mM IPTG and then plated on LB agar supplemented with 20 µg/mL of kanamycin. Mutations were validated using PCR.

To cure isolated mutants of the pMMB67EH^{TetR}::REC$_{Ab}$ plasmid after mutant isolation, strains were streaked for isolated colonies on LB Miller agar supplemented with 2 mM $NiCl_2$ to select cells that had lost the tetracycline cassette (48–51). Cured insertion mutants were then electroporated with pMMB67EH^{TetR} carrying the FLP recombinase. Cells were recovered for 1 hour in 5 mL of LB Miller broth and plated on LB agar containing 10µg/mL of tetracycline and 2 mM IPTG to induce expression of the FLP recombinase. Excision of the kanamycin cassette was confirmed by PCR.

To complement the *A. baumannii* ATCC 17978 mutants, the coding sequence from *A1S_0889* (*olsB*) was cloned into the KpnI/SalI sites, while the coding sequence from *A1S_3376* (*phoR*) was cloned into the KpnI/BamHI sites in pMMB67EH^{KanR}. Plasmids were expressed in the respective mutants, and all strains were grown in 30 µg/mL of kanamycin and 1 mM IPTG for expression.

Analysis of total lipids and aminolipids. Overnight cultures were used to inoculate 10 mL minimal medium 1 mM phosphate, or 20 mL minimal medium 50 µM phosphate to achieve an OD_{600} of ~0.05, and then incubated for 24 hours at 37 ºC. After the incubation period, cells were collected by centrifugation. Lipids were extracted using the Bligh and Dyer (1959) method (52). The chloroform phase was separated into the individual components on high-performance TLC silica gel plates. For one-dimensional TLC analysis, the plates were developed with chloroform-methanol-water (130:50:8 v/v) mixture. For two-dimensional TLC analysis, a chloroform-methanol-water (140:60:10 v/v) mixture was used in the first dimension and chloroform-methanol-acetic acid (130:50:20 v/v) mixture was used in the second dimension. Lipids on TLC were visualized by treating the plates with 10% sulfuric acid in ethanol at 150ºC (total lipids) or 0.2% ninhydrin in acetone at 100ºC (aminolipids).

Analysis of ^{32}P-labeled phospholipids. Overnight cultures were diluted to an OD_{600} of ~0.05 in 10 mL LB Miller broth supplemented with 5 µCi/mL ^{32}P ortho-phosphoric acid (PerkinElmer) and grown until reaching an OD_{600} of ~0.6. After harvesting the cells, lipid extraction was performed using Bligh and Dyer method (52), followed by analysis using TLC as previously described. Subsequently, the TLC plates were dried, exposed to a phosphorimaging screen, and scanned using an Amersham Typhoon laser scanner.

Liquid chromatography: Aminolipids were separated by reversed phase liquid chromatography (LC) using an Acquity UPLC CSH C18 column (pore size 130 Å, 1.7 µm particle size, 2.1 mm × 100 mm, Waters) integrated with a Dionex Ultimate 3000 UHPLC system (Thermo Fisher Scientific). Mobile phases A and B were comprised of methanol:

water: acetonitrile (3:4:3) and isopropanol: water: acetonitrile (90:2.5:7.5), respectively, each containing 10 mM ammonium formate. Dried lipid content from TLC separations and Bligh and Dyer extractions were resuspended in 50:50 mobile phase A: B at a concentration of ~100 ng/uL. A 9 uL injection volume was used, and the column compartment was maintained at a temperature of 50 °C. Aminolipids were separated at a flow rate of 0.275 mL/min with the following gradient: hold at 10% B (0-1 min), 10-45% B (1-5 min), 45-70% B (5-23 min), 70-95% B (23-24 min), hold at 95% B (24-29 min), 95-10% B (29-29.5), and hold at 10% B (29.5-35 min).

Untargeted LC-MS with HCD and Targeted LC-MS with UVPD Experiments: An untargeted negative-ionization mode LC-MS-HCD method was utilized to screen lipid extracts on a Thermo Scientific Orbitrap Fusion Lumos Tribrid mass spectrometer via heated electrospray ionization. Various source parameters included a spray voltage of -3800 V, sheath gas setting of 5, aux gas setting of 10, and ion transfer tube temperature of 300 °C. MS1 data was collected at a resolution of 30,000 at *m/z* 200 in the orbitrap analyzer with a scan range of *m/z* 500-1000, RF lens of 80%, and an AGC target of 5E5. A data dependent acquisition method was used in which the five most abundant ions above an intensity threshold of 5E4 were selected for MS/MS analysis with HCD. Species were isolated using a 1 *m/z* window and subjected to an HCD collision energy of 22%. MS2 spectra were acquired at a resolution of 30,000 at *m/z* 200 in the orbitrap, q-value of 0.1, AGC target of 1E5, maximum injection time of 250 ms, and 2 microscans/scan. Data was manually interpreted using Thermo Xcaliber Qual Browser.

A targeted positive-ionization mode LC-MS/MS method was performed on a Thermo Scientific Orbitrap Eclipse Tribrid mass spectrometer equipped with an ArF excimer laser

(Coherent, Inc.) for 193 nm UVPD. The heated electrospray ionization source was operated at +3800 V, and the source parameters described above were implemented. MS/MS scans with UVPD were acquired in a data dependent manner, with 5 scans collected between each MS1 master scan and an intensity threshold set at 5E4. A targeted mass filter was employed that included the *m/z* values and start/end retention times for unsaturated aminolipids identified from the negative-ionization mode LC-MS with HCD run (with a 15-ppm error tolerance). Aminolipids were isolated with a 1 *m/z* window and activated with 4 laser pulses at 2 mJ/pulse for double bond localization. MS^2 spectra were acquired at a resolution of 30,000 at *m/z* 200 in the orbitrap analyzer, q-value of 0.1, AGC target of 5E5, maximum injection time of 500 ms, and 5 microscans/scan.

RNA sequencing. Transcriptome sequencing analysis was performed as described previously, with modification (50). Briefly, total RNA was extracted from *A. baumannii* ATCC 17978 cultures grown in minimal medium supplemented with either excess (1 mM) or limiting (50 μM) phosphate at OD_{600} of ~0.5 in triplicate, utilizing the Direct-Zol RNA miniprep kit (Zymo Research). Genomic DNA contamination was eliminated using the Turbo DNA-free DNA removal kit (Invitrogen). DNAase-treated RNA samples were then forwarded to SeqCenter for sequencing on the Illumina NextSeq 550 sequencing. Subsequently, the CLC Genomic Workbench software (Qiagen) was employed to map the obtained sequencing data to the *A. baumannii* ATCC 17978 genome annotations and determine the read per kilobase per million (RPKM) expression values and determine the weighted-proportions fold changes in expression values between excess or limitation phosphate conditions. Data were analyzed and plotted using GraphPad Prism software. Data Accession #: GSE276010.

Microscopy and image analysis. Cells were grown as stated above and fixed with paraformaldehyde (PFA) and mounted on 1.5% agarose in 1X phosphate-buffered saline (PBS). Imaging was performed using a Nikon Eclipse Ti-2 wide-field epifluorescence microscope equipped with a Photometrics Prime 95B camera and a Plan Apo 100x, 1.45 numerical aperture objective lens. Images were captured using NIS Elements software. Image analysis was conducted using the microbeJ plugin of ImageJ software.

LOS staining and analysis. All cultures were grown in test tubes containing 5 mL of minimal medium with either excess (1 mM) or limiting (50 µM) phosphate at 37°C in a shaker overnight. For the complementation strains, 30 µg/mL kanamycin and 1 mM IPTG were added. The OD_{600} of the overnight cultures was measured and normalized to OD_{600} of ~1. The cells were then centrifuged at 15,000 rpm for 5 minutes. Each pellet was resuspended in 100 µl of 1X Sample Buffer (4X LDS Sample Buffer, 4% β-mercaptoethanol, and water) and boiled in water for 10 minutes. After cooling, proteinase K was added to each sample and mixed. The samples were then incubated in a 55°C water bath overnight. The following day, the samples were boiled in water for 5 minutes and SDS-PAGE was performed. The gel was then fixed and treated according to the protocol in the Pro-Q Emerald 300 Lipopolysaccharide Gel Stain Kit by Thermo Fisher Scientific (P20495).

Colistin susceptibility assays. Overnight cultures were diluted to OD_{600} ~0.150 in minimal medium supplemented with either excess (1 mM) or limiting (50 µM) phosphate containing 5 mg/L colistin. Each culture, comprising 15 mL, was incubated in 125 mL Erlenmeyer flasks

535 at 37ºC with agitation at 250 rpm. Survivors were analyzed at specific time points by serial
536 dilution plating on LB agar.

537

538 **Acknowledgments**

539 The work was supported by funding from the National Institutes of Health (grants
540 R35GM143053 and R01AI168159 to J.M.B and R35GM139658 to J.S.B), and the Robert A.
541 Welch Foundation (F-1155 to J.S.B.).

542

543

544 **References**

545 1. Raetz CRH, Whitfield C. Lipopolysaccharide endotoxins. *Annu Rev Biochem.*
546 2002;71:635–700.

547 2. Sohlenkamp C, Geiger O. Bacterial membrane lipids: diversity in structures and
548 pathways. *FEMS Microbiol Rev*. 2016 Jan;40(1):133–59.

549 3. Geiger O, González-Silva N, López-Lara IM, Sohlenkamp C. Amino acid-containing
550 membrane lipids in bacteria. *Prog Lipid Res*. 2010 Jan;49(1):46–60.

551 4. Moore EK, Hopmans EC, Rijpstra WIC, Villanueva L, Damsté JSS. Elucidation and
552 identification of amino acid containing membrane lipids using liquid
553 chromatography/high-resolution mass spectrometry. *Rapid Commun Mass Spectrom*
554 *RCM*. 2016 Mar 30;30(6):739–50.

555 5. Vences-Guzmán MÁ, Geiger O, Sohlenkamp C. Ornithine lipids and their structural
556 modifications: from A to E and beyond. *FEMS Microbiol Lett*. 2012 Oct;335(1):1–10.

557 6. Geiger O, Röhrs V, Weissenmayer B, Finan TM, Thomas-Oates JE. The regulator gene
558 phoB mediates phosphate stress-controlled synthesis of the membrane lipid
559 diacylglyceryl-N,N,N-trimethylhomoserine in *Rhizobium (Sinorhizobium) meliloti*. *Mol*
560 *Microbiol*. 1999 Apr;32(1):63–73.

561 7. Dees C, Shively JM. Localization of quantitation of the ornithine lipid of *Thiobacillus*
562 *thiooxidans*. *J Bacteriol*. 1982 Feb;149(2):798–9.

563 8. Palacios-Chaves L, Conde-Álvarez R, Gil-Ramírez Y, Zúñiga-Ripa A, Barquero-Calvo
564 E, Chacón-Díaz C, et al. *Brucella abortus* ornithine lipids are dispensable outer

membrane components devoid of a marked pathogen-associated molecular pattern. *PloS One*. 2011 Jan 7;6(1):e16030.

9. Vences-Guzmán MÁ, Guan Z, Ormeño-Orrillo E, González-Silva N, López-Lara IM, Martínez-Romero E, et al. Hydroxylated ornithine lipids increase stress tolerance in *Rhizobium tropici* CIAT899. *Mol Microbiol*. 2011 Mar;79(6):1496–514.

10. Stirrup R, Mausz MA, Silvano E, Murphy A, Guillonneau R, Quareshy M, et al. Aminolipids elicit functional trade-offs between competitiveness and bacteriophage attachment in *Ruegeria pomeroyi. ISME J*. 2023 Mar;17(3):315–25.

11. Weissenmayer B, Gao JL, López-Lara IM, Geiger O. Identification of a gene required for the biosynthesis of ornithine-derived lipids. *Mol Microbiol*. 2002 Aug;45(3):721–33.

12. Gao JL, Weissenmayer B, Taylor AM, Thomas-Oates J, López-Lara IM, Geiger O. Identification of a gene required for the formation of lyso-ornithine lipid, an intermediate in the biosynthesis of ornithine-containing lipids. *Mol Microbiol*. 2004 Sep;53(6):1757–70.

13. Vences-Guzmán MÁ, Guan Z, Escobedo-Hinojosa WI, Bermúdez-Barrientos JR, Geiger O, Sohlenkamp C. Discovery of a bifunctional acyltransferase responsible for ornithine lipid synthesis in *Serratia proteamaculans. Environ Microbiol*. 2015 May;17(5):1487–96.

14. Lewenza S, Falsafi R, Bains M, Rohs P, Stupak J, Sprott GD, et al. The olsA gene mediates the synthesis of an ornithine lipid in *Pseudomonas aeruginosa* during growth under phosphate-limiting conditions, but is not involved in antimicrobial peptide susceptibility. *FEMS Microbiol Lett*. 2011 Jul;320(2):95–102.

15. Barbosa LC, Goulart CL, Avellar MM, Bisch PM, von Kruger WMA. Accumulation of ornithine lipids in *Vibrio cholerae* under phosphate deprivation is dependent on VC0489 (OlsF) and PhoBR system. *Microbiol Read Engl*. 2018 Mar;164(3):395–9.

16. Harding CM, Hennon SW, Feldman MF. Uncovering the mechanisms of *Acinetobacter baumannii* virulence. *Nat Rev Microbiol*. 2018 Feb;16(2):91–102.

17. Rojas-Jiménez K, Sohlenkamp C, Geiger O, Martínez-Romero E, Werner D, Vinuesa P. A ClC chloride channel homolog and ornithine-containing membrane lipids of *Rhizobium tropici* CIAT899 are involved in symbiotic efficiency and acid tolerance. *Mol Plant-Microbe Interact MPMI*. 2005 Nov;18(11):1175–85.

18. González-Silva N, López-Lara IM, Reyes-Lamothe R, Taylor AM, Sumpton D, Thomas-Oates J, et al. The dioxygenase-encoding olsD gene from *Burkholderia cenocepacia* causes the hydroxylation of the amide-linked fatty acyl moiety of ornithine-containing membrane lipids. *Biochemistry*. 2011 Jul 26;50(29):6396–408.

19. Boll JM, Tucker AT, Klein DR, Beltran AM, Brodbelt JS, Davies BW, et al. Reinforcing Lipid A Acylation on the Cell Surface of *Acinetobacter baumannii* Promotes Cationic

602 Antimicrobial Peptide Resistance and Desiccation Survival. *mBio*. 2015;6(3):e00478-
603 00415.

604 20. Boll JM, Crofts AA, Peters K, Cattoir V, Vollmer W, Davies BW, et al. A penicillin-
605 binding protein inhibits selection of colistin-resistant, lipooligosaccharide-deficient
606 *Acinetobacter baumannii. Proc Natl Acad Sci U S A*. 2016 11;113(41):E6228–37.

607 21. Kang KN, Klein DR, Kazi MI, Guérin F, Cattoir V, Brodbelt JS, et al. Colistin
608 heteroresistance in Enterobacter cloacae is regulated by PhoPQ-dependent 4-amino-4-
609 deoxy-l-arabinose addition to lipid A. Mol Microbiol. 2019;111(6):1604–16.

610 22. Murtha AN, Kazi MI, Schargel RD, Cross T, Fihn C, Cattoir V, et al. High-level
611 carbapenem tolerance requires antibiotic-induced outer membrane modifications. *PLoS*
612 *Pathog*. 2022 Feb;18(2):e1010307.

613 23. Ernst CM, Peschel A. Broad-spectrum antimicrobial peptide resistance by MprF-
614 mediated aminoacylation and flipping of phospholipids. *Mol Microbiol*. 2011
615 Apr;80(2):290–9.

616 24. Needham BD, Trent MS. Fortifying the barrier: the impact of lipid A remodelling on
617 bacterial pathogenesis. *Nat Rev Microbiol*. 2013 Jul;11(7):467–81.

618 25. Henderson JC, Zimmerman SM, Crofts AA, Boll JM, Kuhns LG, Herrera CM, et al. The
619 Power of Asymmetry: Architecture and Assembly of the Gram-Negative Outer
620 Membrane Lipid Bilayer. *Annu Rev Microbiol*. 2016 08;70:255–78.

621 26. de Rudder KE, Thomas-Oates JE, Geiger O. Rhizobium meliloti mutants deficient in
622 phospholipid N-methyltransferase still contain phosphatidylcholine. *J Bacteriol*. 1997
623 Nov;179(22):6921–8.

624 27. Raetz CR, Dowhan W. Biosynthesis and function of phospholipids in *Escherichia coli. J*
625 *Biol Chem*. 1990 Jan 25;265(3):1235–8.

626 28. Lopalco P, Stahl J, Annese C, Averhoff B, Corcelli A. Identification of unique cardiolipin
627 and monolysocardiolipin species in *Acinetobacter baumannii. Sci Rep*. 2017 Jun
628 7;7(1):2972.

629 29. Stankeviciute G, Guan Z, Goldfine H, Klein EA. *Caulobacter crescentus* Adapts to
630 Phosphate Starvation by Synthesizing Anionic Glycoglycerolipids and a Novel
631 Glycosphingolipid. *mBio*. 2019 Apr 2;10(2):e00107-19.

632 30. Escobedo-Hinojosa WI, Vences-Guzmán MÁ, Schubotz F, Sandoval-Calderón M,
633 Summons RE, López-Lara IM, et al. OlsG (Sinac_1600) Is an Ornithine Lipid N-
634 Methyltransferase from the Planctomycete *Singulisphaera acidiphila. J Biol Chem*. 2015
635 Jun 12;290(24):15102–11.

636 31. Kim SK, Park SJ, Li XH, Choi YS, Im DS, Lee JH. Bacterial ornithine lipid, a surrogate
637 membrane lipid under phosphate-limiting conditions, plays important roles in bacterial
638 persistence and interaction with host. *Environ Microbiol*. 2018 Nov;20(11):3992–4008.

639 32. Gallagher LA, Ramage E, Weiss EJ, Radey M, Hayden HS, Held KG, et al. Resources
640 for Genetic and Genomic Analysis of Emerging Pathogen *Acinetobacter baumannii. J*
641 *Bacteriol*. 2015 Jun 15;197(12):2027–35.

642 33. Smith AF, Rihtman B, Stirrup R, Silvano E, Mausz MA, Scanlan DJ, et al. Elucidation
643 of glutamine lipid biosynthesis in marine bacteria reveals its importance under
644 phosphorus deplete growth in Rhodobacteraceae. *ISME J.* 2019 Jan;13(1):39–49.

645 34. Hebecker S, Arendt W, Heinemann IU, Tiefenau JHJ, Nimtz M, Rohde M, et al. Alanyl-
646 phosphatidylglycerol synthase: mechanism of substrate recognition during tRNA-
647 dependent lipid modification in *Pseudomonas aeruginosa. Mol Microbiol*. 2011
648 May;80(4):935–50.

649 35. Arendt W, Hebecker S, Jäger S, Nimtz M, Moser J. Resistance phenotypes mediated by
650 aminoacyl-phosphatidylglycerol synthases. J Bacteriol. 2012 Mar;194(6):1401–16.

651 36. Baek JH, Lee SY. Novel gene members in the Pho regulon of *Escherichia coli. FEMS*
652 *Microbiol Lett*. 2006 Nov;264(1):104–9.

653 37. Hsieh YJ, Wanner BL. Global regulation by the seven-component Pi signaling system.
654 *Curr Opin Microbiol*. 2010 Apr;13(2):198–203.

655 38. Gardner SG, McCleary WR. Control of the phoBR Regulon in *Escherichia coli. EcoSal*
656 *Plus*. 2019 Sep;8(2).

657 39. Hankins JV, Madsen JA, Giles DK, Brodbelt JS, Trent MS. Amino acid addition to *Vibrio*
658 *cholerae* LPS establishes a link between surface remodeling in gram-positive and gram-
659 negative bacteria. *Proc Natl Acad Sci U S A*. 2012 May 29;109(22):8722–7.

660 40. Sohlenkamp C, Galindo-Lagunas KA, Guan Z, Vinuesa P, Robinson S, Thomas-Oates J,
661 et al. The lipid lysyl-phosphatidylglycerol is present in membranes of Rhizobium tropici
662 CIAT899 and confers increased resistance to polymyxin B under acidic growth
663 conditions. *Mol Plant-Microbe Interact MPMI*. 2007 Nov;20(11):1421–30.

664 41. Klein S, Lorenzo C, Hoffmann S, Walther JM, Storbeck S, Piekarski T, et al. Adaptation
665 of *Pseudomonas aeruginosa* to various conditions includes tRNA-dependent formation
666 of alanyl-phosphatidylglycerol. *Mol Microbiol*. 2009 Feb;71(3):551–65.

667 42. Ernst CM, Staubitz P, Mishra NN, Yang SJ, Hornig G, Kalbacher H, et al. The bacterial
668 defensin resistance protein MprF consists of separable domains for lipid lysinylation and
669 antimicrobial peptide repulsion. *PLoS Pathog*. 2009 Nov;5(11):e1000660.

670 43. Geiger O, Padilla-Gómez J, López-Lara IM. Bacterial Sphingolipids and Sulfonolipids.
671 In: Geiger O, editor. Biogenesis of Fatty Acids, Lipids and Membranes [Internet]. Cham:

672 Springer International Publishing; 2019 [cited 2024 Jul 2]. p. 123–37. Available from:
673 https://doi.org/10.1007/978-3-319-50430-8_12

674 44. Zhang X, Ferguson-Miller SM, Reid GE. Characterization of ornithine and glutamine
675 lipids extracted from cell membranes of *Rhodobacter sphaeroides. J Am Soc Mass*
676 *Spectrom*. 2009 Feb;20(2):198–212.

677 45. Aygun-Sunar S, Bilaloglu R, Goldfine H, Daldal F. *Rhodobacter capsulatus* OlsA is a
678 bifunctional enzyme active in both ornithine lipid and phosphatidic acid biosynthesis. *J*
679 *Bacteriol*. 2007 Dec;189(23):8564–74.

680 46. Jones RA, Shropshire H, Zhao C, Murphy A, Lidbury I, Wei T, et al. Phosphorus stress
681 induces the synthesis of novel glycolipids in *Pseudomonas aeruginosa* that confer
682 protection against a last-resort antibiotic. *ISME J.* 2021 Nov;15(11):3303–14.

683 47. Tucker AT, Nowicki EM, Boll JM, Knauf GA, Burdis NC, Trent MS, et al. Defining
684 gene-phenotype relationships in *Acinetobacter baumannii* through one-step
685 chromosomal gene inactivation. *mBio*. 2014;5(4):e01313-01314.

686 48. Kang KN, Kazi MI, Biboy J, Gray J, Bovermann H, Ausman J, et al. Septal Class A
687 Penicillin-Binding Protein Activity and ld-Transpeptidases Mediate Selection of
688 Colistin-Resistant Lipooligosaccharide-Deficient *Acinetobacter baumannii. mBio*. 2021
689 Jan 5;12(1):e02185-20.

690 49. Kang KN, Boll JM. PBP1A Directly Interacts with the Divisome Complex to Promote
691 Septal Peptidoglycan Synthesis in *Acinetobacter baumannii. J Bacteriol.* 2022 Dec
692 20;204(12):e0023922.

693 50. Islam N, Kazi MI, Kang KN, Biboy J, Gray J, Ahmed F, et al. Peptidoglycan Recycling
694 Promotes Outer Membrane Integrity and Carbapenem Tolerance in *Acinetobacter*
695 *baumannii. mBio*. 2022 Jun 28;13(3):e0100122.

696 51. Podolsky T, Fong ST, Lee BT. Direct selection of tetracycline-sensitive *Escherichia coli*
697 cells using nickel salts. *Plasmid*. 1996 Sep;36(2):112–5.

698 52. Bligh EG, Dyer WJ. A rapid method of total lipid extraction and purification. *J Biochem*
699 *Physiol.* 1959 Aug;37(8):911–7.

700

701

702

703

704

Figures

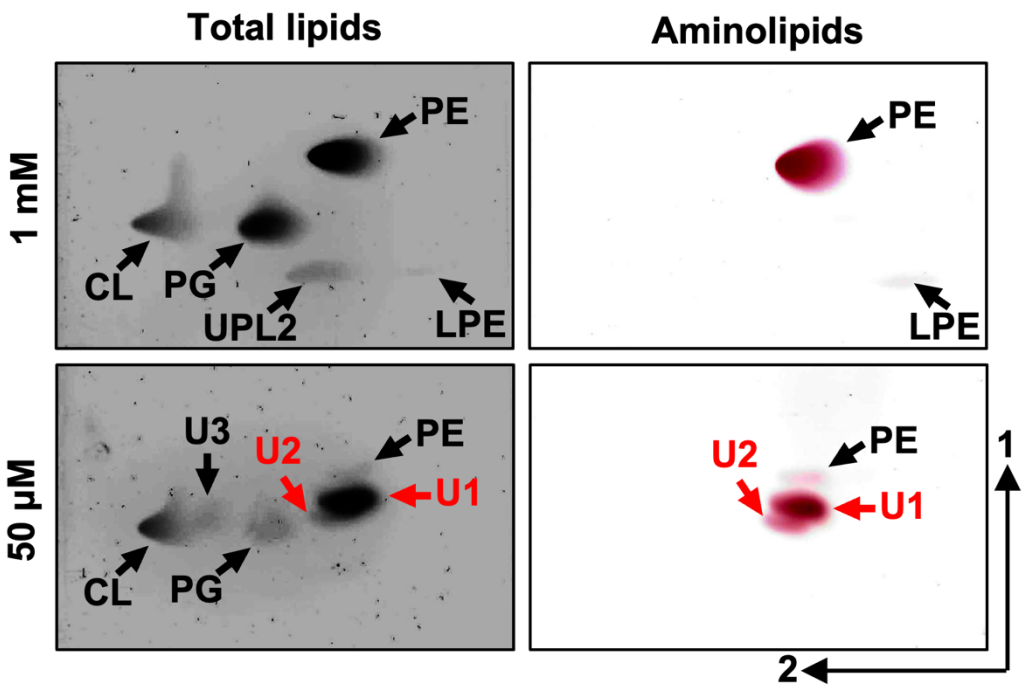

Figure 1: Lipid composition of *A. baumannii* strain ATCC 17978 in excess and limiting phosphate concentrations. Strains were grown in minimal with excess (1 mM) or limiting (50 µM) phosphate. Cells were collected, lipids were extracted using the Bligh and Dyer method and separated using 2-dimensional thin-layer chromatography. Total lipids were stained with sulfuric acid (left). Aminolipids were stained using ninhydrin (right). Specific lipids are labelled: PE, phosphatidylethanolamine; PG, phosphatidylglycerol; CL, cardiolipin; LPE, lyso-PE; U1, unknown lipid 1; U2, unknown lipid 2; U3, unknown lipid 3; UPL2, unknown phospholipid 2. Red letters denote aminolipids that provide the focus of the study.

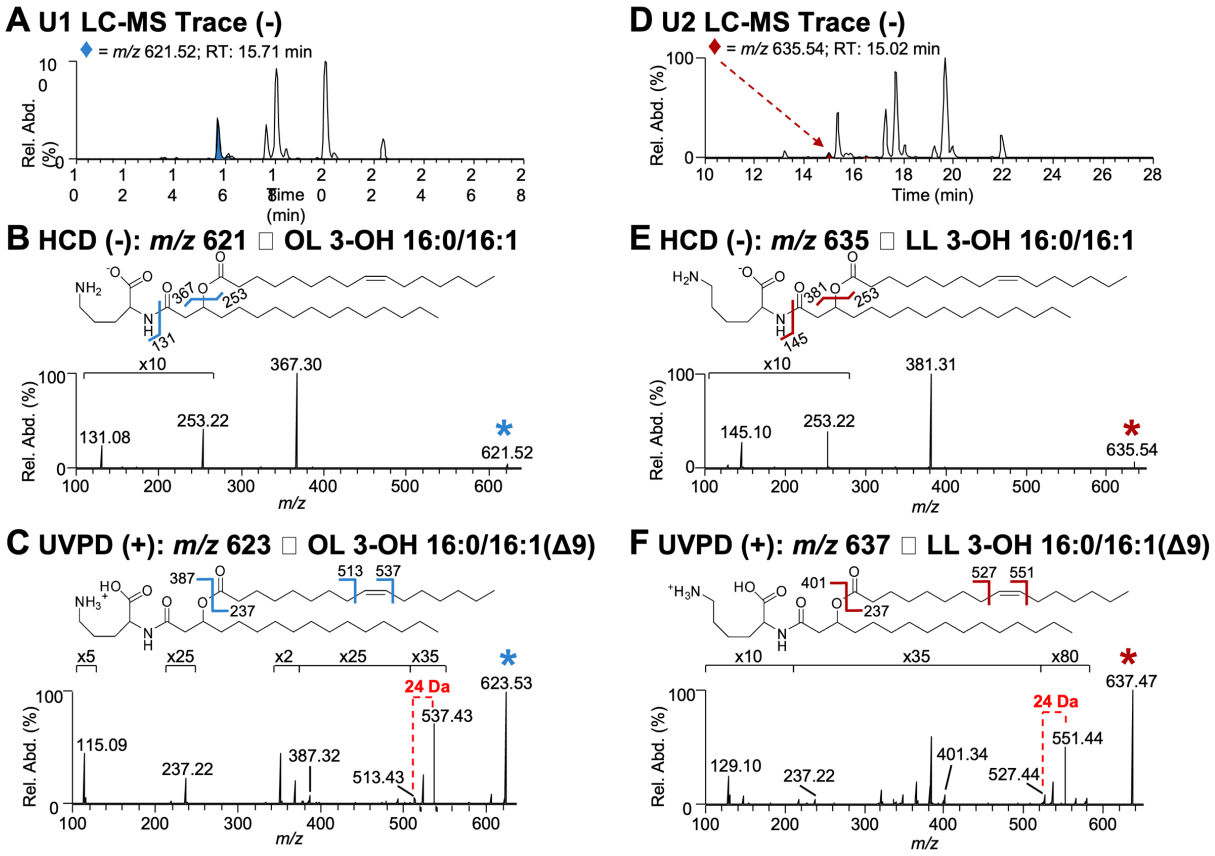

Figure 2: Structural analysis of the lipids produced during phosphate limitation. A. LC-MS trace of U1 lipid extract in negative ionization mode. **B.** HCD (NCE 22) mass spectrum of *m/z* 621.52 ($[M-H]^-$), an ornithine lipid found in U1 extract**. C.** UVPD (4 pulses at 2 mJ/pulse) mass spectrum of *m/z* 623.53 ($[M+H]^+$). **D.** LC-MS trace of U2 lipid extract in negative ionization mode. **E.** HCD (NCE 22) mass spectrum of *m/z* 635.54 ($[M-H]^-$), a lysine lipid found in U2 extract. **F.** UVPD (4 pulses at 2 mJ/pulse) mass spectrum of *m/z* 637.47 ($[M+H]^+$). The selected precursor ions are labeled with asterisks in B,C,E, and F.

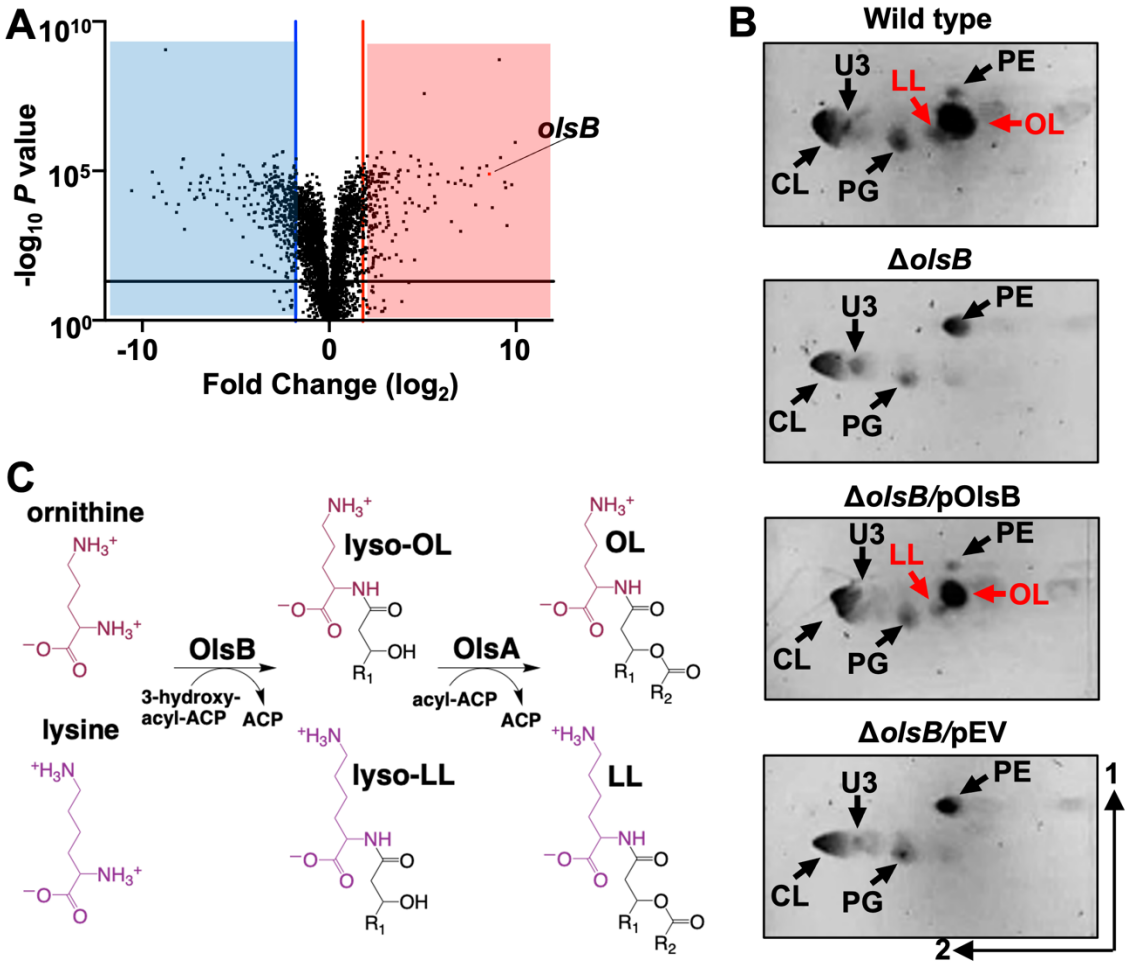

Figure 3: The *olsB* gene is required for ornithine and lysine lipid formation in phosphate limited growth conditions. A. Volcano plot of differentially regulated genes in excess and limiting phosphate. Red/blue lines indicate 3-fold cutoffs. The Black line on the *x*-axis indicates $P < 0.05$. A red dot representing the *olsB* expression profile is shown. **B.** 2D thin-layer chromatography stained with sulfuric acid showing wild type and Δ*olsB* strains grown in phosphate limiting (50 µM) conditions. Specific lipids are labelled: PE, phosphatidylethanolamine; PG, phosphatidylglycerol; CL, cardiolipin; OL, ornithine lipid; LL, lysine lipid; U3, unknown lipid 3. OL and LL aminolipids are labelled in red. **C.** Proposed ornithine lipid (OL) and lysine lipid (LL) biosynthesis pathways in *A. baumannii*.

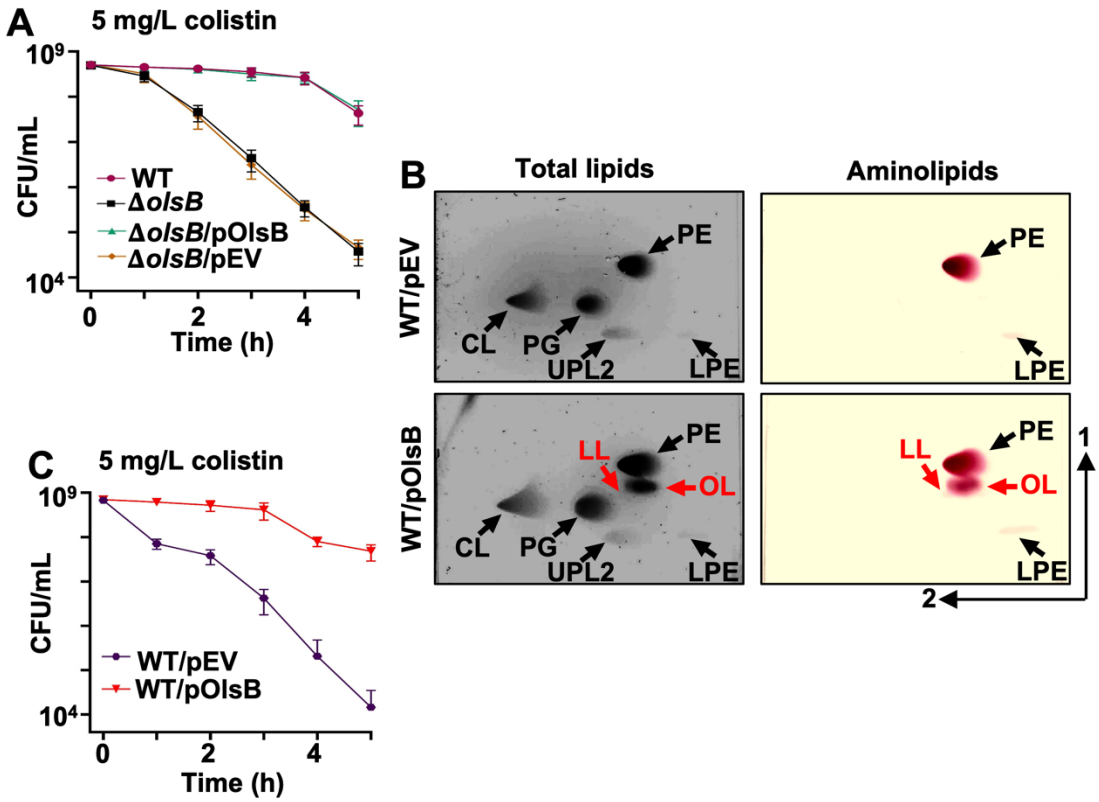

Figure 4: Aminolipids promote colistin tolerance in *A. baumannii*. **A.** Colistin-dependent killing in wild type and Δ*olsB* mutant strains. $n = 3$. Error bars indicate standard deviation. Wild type (WT) strains carrying pOlsB or empty vector were subjected to 5 mg/L colistin exposure over time. CFU/mL were calculated every 0.5 h. **B.** Total lipids were extracted using the Bligh and Dyer method and separated using 2D thin-layer chromatography. Lipids were stained with sulfuric acid (left). Aminolipids were stained using ninhydrin (right). Specific lipids are labelled: PE, phosphatidylethanolamine; PG, phosphatidylglycerol; CL, cardiolipin; LPE, lyso-phosphatidylethanolamine; LL, lysine lipid; OL, ornithine lipid; U3, unknown lipid 3. OL and LL are labelled in red. **C.** Colistin-dependent kill curves (left) and growth rate analysis (right) in wild type expressing empty vector (pEV) or pOlsB ($n = 3$). Error bars indicate standard deviation.

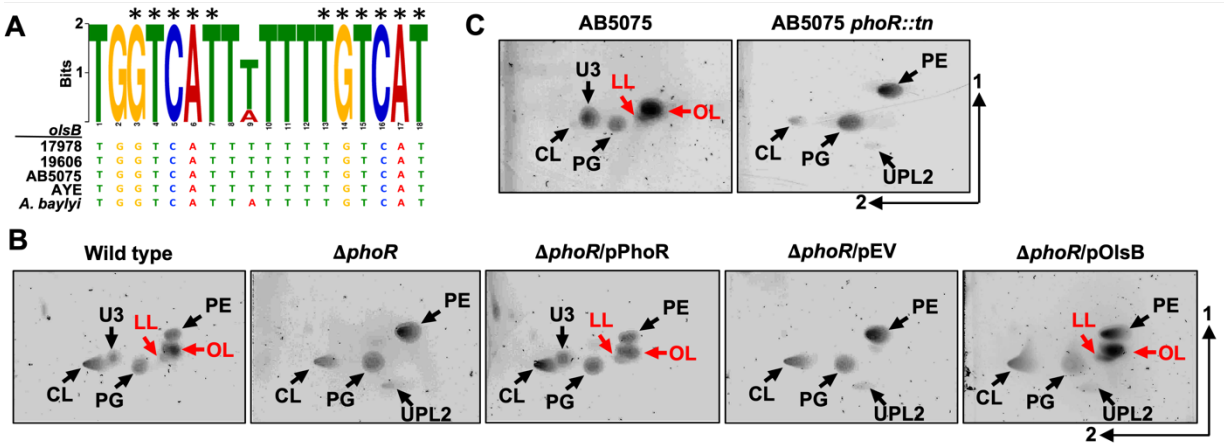

Figure 5: PhoR regulates *olsB* gene expression and aminolipid formation in *A. baumannii* strains. **A.** Predicted Pho box sequence alignments from *A. baumannii* strain 17978, 19606, AB5075, AYE, and *A. baylyi olsB* promoters. Black asterisks represent conserved nucleotides in the *E. coli* Pho box consensus (CT*GTCAT*NNNNC*TGTCAT*). **B.** 2D thin-layer chromatography lipid analysis from *A. baumannii* strain ATCC 17978 wild type and mutants grown in minimal media supplemented with 50 µM (limiting) phosphate. **C.** 2D thin-layer chromatography lipid analysis from *A. baumannii* strain AB5075 wild type and the *phoR* Tn*26* mutant in minimal media supplemented with 50 µM (limiting) phosphate. Lipids were stained with sulfuric acid. OL and LL aminolipids are labelled in red.

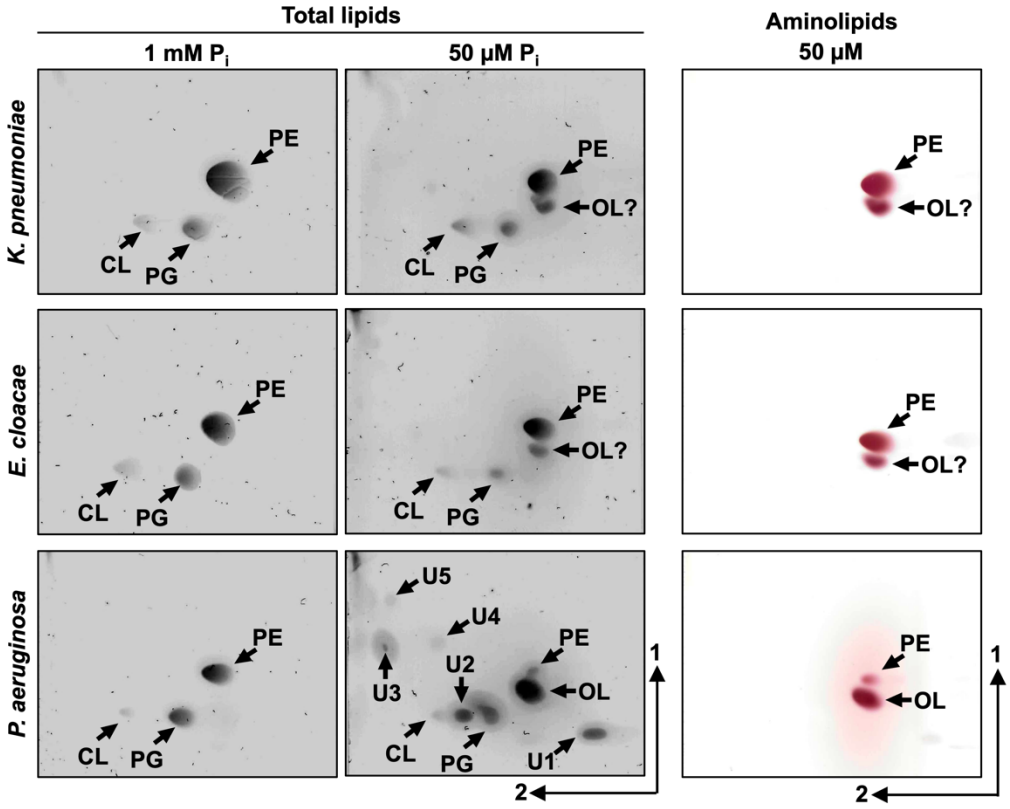

Figure 6: Aminolipid biosynthesis is conserved in Gram-negative ESKAPE pathogens. 2D thin-layer chromatography of lipids extracted from wild type *K. pneumoniae* strain KPNIH1, *E. cloacae* strain ATCC 13047, and *P. aeruginosa* strain PAO1 grown in excess (1 mM) or limiting (50 µM) phosphate conditions. Totals lipids were stained with sulfuric acid (left). Aminolipids were stained using ninhydrin (right). Specific lipids are labelled: PE, phosphatidylethanolamine; PG, phosphatidylglycerol; CL, cardiolipin; OL, ornithine lipid; U1, U2, U3, U4, and U5; unknown compounds 1, 2, 3, 4, and 5.

Supplementary Captions

Figure S1: *Escherichia coli* (*Ec*) and *Acinetobacter baumannii (Ab)* lipid composition after growth in complex media.

Figure S2: Effect of phosphate availability on growth, cell morphology, and LOS production.

Figure S3: Thin-layer chromatography of aminolipids in *Acinetobacter* strains.

Figure S4: *olsB* and *olsA* are required for ornithine and lysine lipid biosynthesis in *A. baumannii*.

Figure S5: Aminolipid formation promotes *A. baumannii* tolerance to colistin.

Table S1: Identity of aminolipids in U1 biological replicates.

Table S2: Identity of aminolipids in U2 biological replicates.

Table S3: Differentially regulated genes in excess and limiting phosphate.

Table S4: Strains and plasmids used in this study.

Table S5: Primers used in this study.